Recurrent Neural Network Adaptive Control of Wing-Rock Motion

Chih-Min Lin* and Chun-Fei Hsu†
Yuan-Ze University,
Chung-Li 320, Taiwan, Republic of China

I. Introduction

SOME combat aircraft often operate at subsonic speeds and high angles of attack. These aircraft may become unstable due to oscillation, mainly a rolling motion known as wing-rock motion.[1] This wing-rock motion is a concern because it may have adverse effects on maneuverability, tracking accuracy, and operational safety. However, the underlying mechanism of the wing-rock motion is not clearly understood. Some analytical studies have been performed to understand the dynamics of the wing rock.[2,3] Moreover, a series of papers have considered the control of the wing-rock motion system based on the adaptive control technique.[4,5] The adaptive control requires knowledge of the structure of the aerodynamic functions; however, this structure is difficult to obtain. In addition, a neural network (NN) adaptive controller has been proposed to learn the system dynamic function.[4] However, the NN must be selected with a sufficiently large number of neurons in the hidden layer, which consumes a large amount of processing time for real-time applications. Moreover, the NN presented in Ref. 4 is a feedforward NN belonging to static mapping networks. On the other hand, a recurrent NN (RNN) has advantages over a feedforward NN, such as its dynamic response and its information storing ability.[6] Because an RNN has an internal feedback loop, it captures the dynamic response of system with external feedback through delays. Thus, the RNN is a dynamic mapping network.

In this Note, an RNN adaptive control system is developed for a wing-rock motion system. The RNN adaptive control system comprises an RNN controller and a compensation controller. The RNN controller is the principal controller, and the compensation controller is a compensator for the difference between the system dynamic and the RNN approximator. Because the RNN system uses an internal feedback loop, its learning capability is superior to the feedforward NN for dynamic response. Moreover, the Taylor linearization technique is employed to increase the learning ability of the RNN. The online parameter adaptation laws are derived based on a Lyapunov function; thus, the stability of the system can be guaranteed.

II. Problem Statement and Control Objective

The aerodynamic rolling moment is a complex nonlinear function of the roll angle, roll rate, and angle of attack. By defining the state vector $\boldsymbol{x} = [x_1, x_2]^T = [\phi, \dot{\phi}]^T$, where ϕ is the roll angle, a dynamic system of the wing-rock motion system can be written in a state variable form as[4]

$$\dot{x}_1 = x_2, \qquad \dot{x}_2 = f(\boldsymbol{x}) + u \tag{1}$$

where

$$f(\boldsymbol{x}) = b_0 + b_1 x_1 + b_2 x_2 + b_3|x_1|x_2 + b_4|x_2|x_2 + b_5 x_1^3 \tag{2}$$

and the parameters b_i, $i = 0, 1, \ldots, 5$ are nonlinear functions of the angle of attack. A reference model is specified by a linear time-invariant differential equation

$$\dot{\boldsymbol{x}}_m = \boldsymbol{A}_m \boldsymbol{x}_m \tag{3}$$

where $\boldsymbol{x}_m = [x_{m1}, x_{m2}]^T = [\phi_m, \dot{\phi}_m]^T$ is the reference trajectory vector and

$$\boldsymbol{A}_m = \begin{bmatrix} 0 & 1 \\ -\omega_n^2 & -2\xi\omega_n \end{bmatrix} \tag{4}$$

where $\xi > 0$ is the damping ratio and $\omega_n > 0$ is the natural frequency. For the choice of the damping ratio and natural frequency, $\boldsymbol{A}_m$ is a Hurwitz matrix and the reference trajectory vector $\boldsymbol{x}_m$ starting from any nonzero initial condition tends to zeros as $t \to \infty$. Define the trajectory tracking error $\boldsymbol{e} = \boldsymbol{x} - \boldsymbol{x}_m = [\phi - \phi_m, \dot{\phi} - \dot{\phi}_m]^T$. Then, the error dynamic is given by

$$\dot{\boldsymbol{e}} = \boldsymbol{A}_m \boldsymbol{e} + \boldsymbol{d}_m[g(\boldsymbol{x}) + u] \tag{5}$$

where

$$\boldsymbol{d}_m = [0, 1]^T \tag{6}$$

$$g(\boldsymbol{x}) = b_0 + \left(b_1 + \omega_n^2\right)x_1 + (b_2 + 2\xi\omega_n)x_2 + b_3|x_1|x_2 + b_4|x_2|x_2 + b_5 x_1^3 \tag{7}$$

III. RNN Adaptive Controller Design

If the nonlinear function $g(\boldsymbol{x})$ is accurately known, there exists an ideal controller $u^* = -g(\boldsymbol{x})$ such that Eq. (5) becomes $\dot{\boldsymbol{e}} = \boldsymbol{A}_m \boldsymbol{e}$. Because $\boldsymbol{A}_m$ is a Hurwitz matrix, this implies $\lim_{t\to\infty} \boldsymbol{e} = \boldsymbol{0}$. However, because the nonlinear function $g(\boldsymbol{x})$ cannot be accurately known, the ideal controller u^* cannot be exactly implemented. To solve this problem, an RNN is utilized to approximate the system dynamic function $g(\boldsymbol{x})$. By the universal approximation theorem, there exists an optimal RNN approximator g^* such that[7]

$$g(\boldsymbol{x}) = g^*(\boldsymbol{x}, \boldsymbol{c}^*, \boldsymbol{s}^*, \boldsymbol{r}^*, \boldsymbol{w}^*) + \Delta = \boldsymbol{w}^{*T}\boldsymbol{\theta}^*(\boldsymbol{x}, \boldsymbol{c}^*, \boldsymbol{s}^*, \boldsymbol{r}^*) + \Delta \tag{8}$$

where Δ denotes an approximation error; $\boldsymbol{w}^*$ and $\boldsymbol{\theta}^*$ are the optimal parameter vectors of $\boldsymbol{w}$ and $\boldsymbol{\theta}$, respectively; and $\boldsymbol{c}^*$, $\boldsymbol{s}^*$, and $\boldsymbol{r}^*$ are the optimal parameter vectors of $\boldsymbol{c}$, $\boldsymbol{s}$, and $\boldsymbol{r}$, where the vectors $\boldsymbol{c}$, $\boldsymbol{s}$, and $\boldsymbol{r}$ collect the parameters of the center and inverse radius of the radial basis function and the internal feedback gain of an RNN, respectively.[6] The RNN approximator is defined as

$$\hat{g} = \hat{\boldsymbol{w}}^T \hat{\boldsymbol{\theta}}(\boldsymbol{x}, \hat{\boldsymbol{c}}, \hat{\boldsymbol{s}}, \hat{\boldsymbol{r}}) \tag{9}$$

where $\hat{\boldsymbol{w}}$ and $\hat{\boldsymbol{\theta}}$ are the estimated vectors of $\boldsymbol{w}^*$ and $\boldsymbol{\theta}^*$, respectively, and $\hat{\boldsymbol{c}}$, $\hat{\boldsymbol{s}}$, and $\hat{\boldsymbol{r}}$ are the estimated vectors of $\boldsymbol{c}^*$, $\boldsymbol{s}^*$, and $\boldsymbol{r}^*$, respectively. Define the estimated error $\tilde{g}$ as

$$\tilde{g} = g - \hat{g} = g^* - \hat{g} + \Delta = \tilde{\boldsymbol{w}}^T \hat{\boldsymbol{\theta}} + \hat{\boldsymbol{w}}^T \tilde{\boldsymbol{\theta}} + \tilde{\boldsymbol{w}}^T \tilde{\boldsymbol{\theta}} + \Delta \tag{10}$$

where $\tilde{\boldsymbol{w}} = \boldsymbol{w}^* - \hat{\boldsymbol{w}}$ and $\tilde{\boldsymbol{\theta}} = \boldsymbol{\theta}^* - \hat{\boldsymbol{\theta}}$. In the following, some adaptive laws will be derived to online tune the center, inverse radius, and feedback gain of the RNN approximator to achieve favorable estimation of the dynamic function. To achieve this goal, the Taylor expansion linearization technique is employed to transform the nonlinear radial basis function into a partially linear form, that is,

$$\tilde{\boldsymbol{\theta}} = \begin{bmatrix} \tilde{\theta}_1 \\ \tilde{\theta}_2 \\ \vdots \\ \tilde{\theta}_n \end{bmatrix} = \begin{bmatrix} \dfrac{\partial \Theta_1}{\partial \boldsymbol{c}} \\ \dfrac{\partial \Theta_2}{\partial \boldsymbol{c}} \\ \vdots \\ \dfrac{\partial \Theta_n}{\partial \boldsymbol{c}} \end{bmatrix} \Bigg|_{c=\hat{c}} \tilde{\boldsymbol{c}} + \begin{bmatrix} \dfrac{\partial \Theta_1}{\partial \boldsymbol{s}} \\ \dfrac{\partial \Theta_2}{\partial \boldsymbol{s}} \\ \vdots \\ \dfrac{\partial \Theta_n}{\partial \boldsymbol{s}} \end{bmatrix} \Bigg|_{s=\hat{s}} \tilde{\boldsymbol{s}} + \begin{bmatrix} \dfrac{\partial \Theta_1}{\partial \boldsymbol{r}} \\ \dfrac{\partial \Theta_2}{\partial \boldsymbol{r}} \\ \vdots \\ \dfrac{\partial \Theta_n}{\partial \boldsymbol{r}} \end{bmatrix} \Bigg|_{r=\hat{r}} \tilde{\boldsymbol{r}} + \boldsymbol{H} \tag{11}$$

Received 8 January 2002; revision received 2 July 2002; accepted for publication 29 July 2002.

*Professor, Department of Electrical Engineering; cml@ee.yzu.edu.tw.
†Graduate Student, Department of Electrical Engineering.

or

$$\tilde{\boldsymbol{\theta}} = \boldsymbol{A}^T\tilde{\boldsymbol{c}} + \boldsymbol{B}^T\tilde{\boldsymbol{s}} + \boldsymbol{C}^T\tilde{\boldsymbol{r}} + \boldsymbol{H} \tag{12}$$

where

$$\boldsymbol{A} = \left[\frac{\partial\Theta_1}{\partial\boldsymbol{c}} \cdots \frac{\partial\Theta_n}{\partial\boldsymbol{c}}\right]\Big|_{c=\hat{c}}, \qquad \boldsymbol{B} = \left[\frac{\partial\Theta_1}{\partial\boldsymbol{s}} \cdots \frac{\partial\Theta_n}{\partial\boldsymbol{s}}\right]\Big|_{s=\hat{s}}$$

$$\boldsymbol{C} = \left[\frac{\partial\Theta_1}{\partial\boldsymbol{r}} \cdots \frac{\partial\Theta_n}{\partial\boldsymbol{r}}\right]\Big|_{r=\hat{r}}$$

$\boldsymbol{H}$ is a vector of higher-order terms; $\tilde{\boldsymbol{c}} = \boldsymbol{c}^* - \hat{\boldsymbol{c}}$, $\tilde{\boldsymbol{s}} = \boldsymbol{s}^* - \hat{\boldsymbol{s}}$, and $\tilde{\boldsymbol{r}} = \boldsymbol{r}^* - \hat{\boldsymbol{r}}$; and $\partial\Theta_k/\partial\boldsymbol{c}$, $\partial\Theta_k/\partial\boldsymbol{s}$, and $\partial\Theta_k/\partial\boldsymbol{r}$ are defined as

$$\left[\frac{\partial\Theta_k}{\partial\boldsymbol{c}}\right]^T = \left[\underset{(k-1)\times m}{0\cdots0}\ \frac{\partial\Theta_k}{\partial c_{1k}} \cdots \frac{\partial\Theta_k}{\partial c_{mk}}\ \underset{(n-k)\times m}{0\cdots0}\right] \tag{13}$$

$$\left[\frac{\partial\Theta_k}{\partial\boldsymbol{s}}\right]^T = \left[\underset{(k-1)\times m}{0\cdots0}\ \frac{\partial\Theta_k}{\partial \boldsymbol{s}_{1k}} \cdots \frac{\partial\Theta_k}{\partial \boldsymbol{s}_{mk}}\ \underset{(n-k)\times m}{0\cdots0}\right] \tag{14}$$

$$\left[\frac{\partial\Theta_k}{\partial\boldsymbol{r}}\right]^T = \left[\underbrace{0\cdots0}_{(k-1)}\frac{\partial\Theta_k}{\partial r_k}\underbrace{0\cdots0}_{(n-k)}\right] \tag{15}$$

By the substitution of Eq. (12) into Eq. (10), it can be determined that

$$\begin{aligned}\tilde{g} &= \tilde{\boldsymbol{w}}^T\hat{\boldsymbol{\theta}} + \hat{\boldsymbol{w}}^T(\boldsymbol{A}^T\tilde{\boldsymbol{c}} + \boldsymbol{B}^T\tilde{\boldsymbol{s}} + \boldsymbol{C}^T\tilde{\boldsymbol{r}} + \boldsymbol{H}) + \tilde{\boldsymbol{w}}^T\tilde{\boldsymbol{\theta}} + \Delta \\ &= \tilde{\boldsymbol{w}}^T\hat{\boldsymbol{\theta}} + \tilde{\boldsymbol{c}}^T\boldsymbol{A}\hat{\boldsymbol{w}} + \tilde{\boldsymbol{s}}^T\boldsymbol{B}\hat{\boldsymbol{w}} + \tilde{\boldsymbol{r}}^T\boldsymbol{C}\hat{\boldsymbol{w}} + \varepsilon \end{aligned} \tag{16}$$

where $\hat{\boldsymbol{w}}^T\boldsymbol{A}^T\tilde{\boldsymbol{c}} = \tilde{c}^T\boldsymbol{A}\hat{\boldsymbol{w}}$, $\hat{\boldsymbol{w}}^T\boldsymbol{B}^T\tilde{\boldsymbol{s}} = \tilde{\boldsymbol{s}}^T\boldsymbol{B}\hat{\boldsymbol{w}}$, and $\hat{\boldsymbol{w}}^T\boldsymbol{C}^T\tilde{\boldsymbol{r}} = \tilde{\boldsymbol{r}}^T\boldsymbol{C}\hat{\boldsymbol{w}}$ are used because they are scales, and the uncertain term $\varepsilon = \hat{\boldsymbol{w}}^T\boldsymbol{H} + \tilde{\boldsymbol{w}}^T\tilde{\boldsymbol{\theta}} + \Delta$ is assumed to be bounded by $|\varepsilon| \le E$ where E is a positive constant.

For the error dynamics presented in Eq. (5), the RNN adaptive control law is proposed as

$$u(t) = u_{\text{RNN}}(t) + u_{\text{cp}}(t) \tag{17}$$

where the RNN controller

$$u_{\text{RNN}}(t) = -\hat{g}(\boldsymbol{x}) = -\hat{\boldsymbol{w}}^T\hat{\boldsymbol{\theta}}(\boldsymbol{x}, \hat{\boldsymbol{c}}, \hat{\boldsymbol{s}}, \hat{\boldsymbol{r}}) \tag{18}$$

and the compensation controller

$$u_{\text{cp}}(t) = -\hat{E}\ \text{sgn}\left(\boldsymbol{e}^T\boldsymbol{P}\boldsymbol{d}_m\right) \tag{19}$$

in which sgn( ) is a sign function. In the RNN controller, the system dynamic function is estimated by the RNN approximator in Eq. (18). In the compensation controller, $\hat{E}$ is an estimated value of the approximation error bound E, and $\boldsymbol{P}$ is a positive matrix. By the substitution of Eqs. (17–19) into Eq. (5), the error dynamic is obtained as

$$\begin{aligned}\dot{\boldsymbol{e}} &= \boldsymbol{A}_m\boldsymbol{e} + \boldsymbol{d}_m[g(\boldsymbol{x}) - \hat{g}(\boldsymbol{x}) + u_{\text{cp}}] = \boldsymbol{A}_m\boldsymbol{e} + \boldsymbol{d}_m\big[\tilde{\boldsymbol{w}}^T\hat{\boldsymbol{\theta}} + \tilde{\boldsymbol{c}}^T\boldsymbol{A}\hat{\boldsymbol{w}} \\ &\quad + \tilde{\boldsymbol{s}}^T\boldsymbol{B}\hat{\boldsymbol{w}} + \tilde{\boldsymbol{r}}^T\boldsymbol{C}\hat{\boldsymbol{w}} + \varepsilon - \hat{E}\ \text{sgn}\left(\boldsymbol{e}^T\boldsymbol{P}\boldsymbol{d}_m\right)\big]\end{aligned} \tag{20}$$

Because $\boldsymbol{A}_m$ is a Hurwitz matrix, given a positive-definite symmetric matrix $\boldsymbol{Q}$ (denoted as $\boldsymbol{Q} > 0$), there exists a matrix $\boldsymbol{P} > 0$ such that a Lyapunov equation

$$\boldsymbol{A}_m^T\boldsymbol{P} + \boldsymbol{P}\boldsymbol{A}_m = -\boldsymbol{Q} \tag{21}$$

is satisfied.

Theorem 1: Consider the wing-rock system presented in Eq. (1). If the RNN adaptive controller is designed as in Eq. (17), in which the compensation controller $\boldsymbol{u}_{\text{cp}}(t)$ is given in Eq. (19) with the bound estimation presented in Eq. (26), and if the RNN controller $\boldsymbol{u}_{\text{RNN}}(t)$ is given in Eq. (18) with the adaptive laws of the approximator given in Eqs. (22–25),

$$\dot{\hat{\boldsymbol{w}}} = -\dot{\tilde{\boldsymbol{w}}} = \eta_1\boldsymbol{e}^T\boldsymbol{P}\boldsymbol{d}_m\hat{\boldsymbol{\theta}} \tag{22}$$

$$\dot{\hat{\boldsymbol{c}}} = -\dot{\tilde{\boldsymbol{c}}} = \eta_2\boldsymbol{e}^T\boldsymbol{P}\boldsymbol{d}_m\boldsymbol{A}\hat{\boldsymbol{w}} \tag{23}$$

$$\dot{\hat{\boldsymbol{s}}} = -\dot{\tilde{\boldsymbol{s}}} = \eta_3\boldsymbol{e}^T\boldsymbol{P}\boldsymbol{d}_m\boldsymbol{B}\hat{\boldsymbol{w}} \tag{24}$$

$$\dot{\hat{\boldsymbol{r}}} = -\dot{\tilde{\boldsymbol{r}}} = \eta_4\boldsymbol{e}^T\boldsymbol{P}\boldsymbol{d}_m\boldsymbol{C}\hat{\boldsymbol{w}} \tag{25}$$

$$\dot{\hat{E}}(t) = -\dot{\tilde{E}}(t) = \eta_5\left|\boldsymbol{e}^T\boldsymbol{P}\boldsymbol{d}_m\right| \tag{26}$$

where η_1, η_2, η_3, η_4, and η_5 are the learning rates with positive constants, then the stability of the system can be guaranteed.

Proof: Define a Lyapunov function as

$$\begin{aligned}V(\boldsymbol{e}, \tilde{\boldsymbol{w}}, \tilde{\boldsymbol{c}}, \tilde{\boldsymbol{s}}, \tilde{\boldsymbol{r}}, \tilde{E}) &= \boldsymbol{e}^T\boldsymbol{P}\boldsymbol{e} + \tilde{\boldsymbol{w}}^T\tilde{\boldsymbol{w}}\big/\eta_1 + \tilde{\boldsymbol{c}}^T\tilde{\boldsymbol{c}}\big/\eta_2 + \tilde{\boldsymbol{s}}^T\tilde{\boldsymbol{s}}\big/\eta_3 \\ &\quad + \tilde{\boldsymbol{r}}^T\tilde{\boldsymbol{r}}\big/\eta_4 + \tilde{E}^2\big/\eta_5\end{aligned} \tag{27}$$

where $\tilde{E}(t) = E - \hat{E}(t)$. When Eq. (27) is differentiated with respect to time, and by the use of Eqs. (20) and (22–26), it is determined that

$$\begin{aligned}\dot{V}(\boldsymbol{e}, \tilde{\boldsymbol{w}}, \tilde{\boldsymbol{c}}, \tilde{\boldsymbol{s}}, \tilde{\boldsymbol{r}}, \tilde{E}) &= \boldsymbol{e}^T\boldsymbol{P}\dot{\boldsymbol{e}} + \dot{\boldsymbol{e}}^T\boldsymbol{P}\boldsymbol{e} + 2\big(\tilde{\boldsymbol{w}}^T\dot{\tilde{\boldsymbol{w}}}\big/\eta_1 + \tilde{\boldsymbol{c}}^T\dot{\tilde{\boldsymbol{c}}}\big/\eta_2 \\ &\quad + \tilde{\boldsymbol{s}}^T\dot{\tilde{\boldsymbol{s}}}\big/\eta_3 + \tilde{\boldsymbol{r}}^T\dot{\tilde{\boldsymbol{r}}}\big/\eta_4 + \tilde{E}\dot{\tilde{E}}\big/\eta_5\big) = \boldsymbol{e}^T\left(\boldsymbol{A}_m^T\boldsymbol{P} + \boldsymbol{P}\boldsymbol{A}_m\right)\boldsymbol{e} \\ &\quad + 2\boldsymbol{e}^T\boldsymbol{P}\boldsymbol{d}_m\big[\tilde{\boldsymbol{w}}^T\hat{\boldsymbol{\theta}} + \tilde{\boldsymbol{c}}^T\boldsymbol{A}\hat{\boldsymbol{w}} + \tilde{\boldsymbol{s}}^T\boldsymbol{B}\hat{\boldsymbol{w}} + \tilde{\boldsymbol{r}}^T\boldsymbol{C}\hat{\boldsymbol{w}} + \varepsilon \\ &\quad - \hat{E}\ \text{sgn}\left(\boldsymbol{e}^T\boldsymbol{P}\boldsymbol{d}_m\right)\big] + 2\big(\tilde{\boldsymbol{w}}^T\dot{\tilde{\boldsymbol{w}}}\big/\eta_1 + \tilde{\boldsymbol{c}}^T\dot{\tilde{\boldsymbol{c}}}\big/\eta_2 + \tilde{\boldsymbol{s}}^T\dot{\tilde{\boldsymbol{s}}}\big/\eta_3 \\ &\quad + \tilde{\boldsymbol{r}}^T\dot{\tilde{\boldsymbol{r}}}\big/\eta_4 + \tilde{E}\dot{\tilde{E}}/\eta_5\big) = -\boldsymbol{e}^T\boldsymbol{Q}\boldsymbol{e} + 2\tilde{\boldsymbol{w}}^T\left(\boldsymbol{e}^T\boldsymbol{P}\boldsymbol{d}_m\hat{\boldsymbol{\theta}} + \dot{\tilde{\boldsymbol{w}}}/\eta_1\right) \\ &\quad + 2\tilde{\boldsymbol{c}}^T\left(\boldsymbol{e}^T\boldsymbol{P}\boldsymbol{d}_m\boldsymbol{A}\hat{\boldsymbol{w}} + \dot{\tilde{\boldsymbol{c}}}/\eta_2\right) + 2\tilde{\boldsymbol{s}}^T\left(\boldsymbol{e}^T\boldsymbol{P}\boldsymbol{d}_m\boldsymbol{B}\hat{\boldsymbol{w}} + \dot{\tilde{\boldsymbol{s}}}/\eta_3\right) \\ &\quad + 2\tilde{\boldsymbol{r}}^T\left(\boldsymbol{e}^T\boldsymbol{P}\boldsymbol{d}_m\boldsymbol{C}\hat{\boldsymbol{w}} + \dot{\tilde{\boldsymbol{r}}}/\eta_4\right) + 2\boldsymbol{e}^T\boldsymbol{P}\boldsymbol{d}_m\big[\varepsilon - \hat{E}\ \text{sgn}\left(\boldsymbol{e}^T\boldsymbol{P}\boldsymbol{d}_m\right)\big] \\ &\quad + 2(\tilde{E}\dot{\tilde{E}}/\eta_5) = -\boldsymbol{e}^T\boldsymbol{Q}\boldsymbol{e} + 2\boldsymbol{e}^T\boldsymbol{P}\boldsymbol{d}_m\big[\varepsilon - \hat{E}\ \text{sgn}\left(\boldsymbol{e}^T\boldsymbol{P}\boldsymbol{d}_m\right)\big] \\ &\quad - 2(E - \hat{E})\left|\boldsymbol{e}^T\boldsymbol{P}\boldsymbol{d}_m\right| = -\boldsymbol{e}^T\boldsymbol{Q}\boldsymbol{e} + 2\varepsilon\boldsymbol{e}^T\boldsymbol{P}\boldsymbol{d}_m - 2E\left|\boldsymbol{e}^T\boldsymbol{P}\boldsymbol{d}_m\right| \\ &\le -\boldsymbol{e}^T\boldsymbol{Q}\boldsymbol{e} + 2|\varepsilon|\left|\boldsymbol{e}^T\boldsymbol{P}\boldsymbol{d}_m\right| - 2E\left|\boldsymbol{e}^T\boldsymbol{P}\boldsymbol{d}_m\right| \le 0\end{aligned}$$

As a result, from the Lyapunov theorem (see Ref. 7), the RNN adaptive control system is guaranteed to be stable.

IV. Simulation Results

The aerodynamic parameters of the delta wing for a 25-deg angle of attack are used for simulation.[4] The b_i parameters for the model in Eq. (2) are given by

$$\begin{aligned}&b_0 = 0, \qquad b_1 = -0.01859521, \qquad b_2 = 0.015162375 \\ &b_3 = -0.06245153, \qquad b_4 = 0.00954708, \qquad b_5 = 0.02145291\end{aligned} \tag{28}$$

The reference trajectory vector is chosen $\boldsymbol{x}_m = 0$ as $t \to \infty$ with the parameters ξ and ω_n chosen as 1 and 0.8, respectively. For a choice of $\boldsymbol{Q} = -\boldsymbol{I}$, solving the Lyapunov equation (21) gives

$$\boldsymbol{P} = \begin{bmatrix}1.7625 & 0.7812 \\ 0.7812 & 0.8088\end{bmatrix} \tag{29}$$

The learning rate constants in Eqs. (22–26) are selected as $\eta_1 = 20$, $\eta_2 = 20$, $\eta_3 = 20$, $\eta_4 = 20$, and $\eta_5 = 0.1$. If the learning rate constants η_i, $i = 1, 2, \ldots, 5$, are chosen to be small, then the parameter convergence of the RNN adaptive controller will be easily achieved; however, this will result in slow learning speed. On the other hand, if the learning rate constants are chosen to be large, then the learning speed will be fast; however, the RNN adaptive controller system may

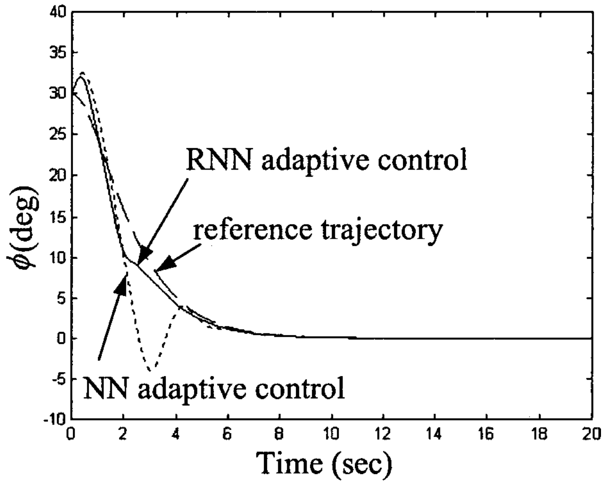

a) State responses

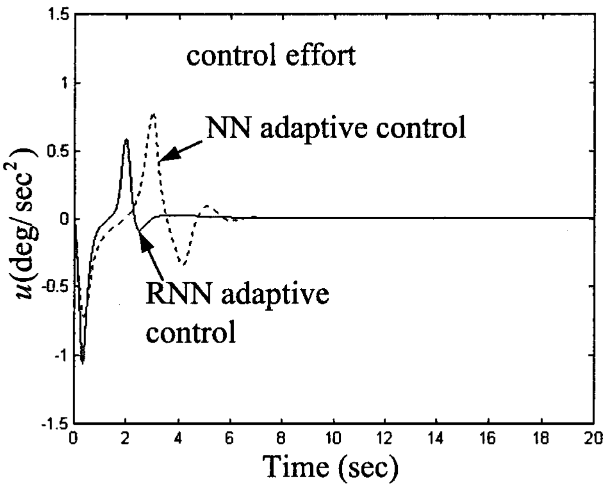

b) Associated control efforts

Fig. 1 NN and RNN adaptive control responses of wing-rock motion.

become more unstable for the parameter convergence. In the following, a comparison of the tracking accuracy is presented by using the NN adaptive controller in Ref. 4 and the proposed RNN adaptive controller. The NN adaptive controller used a traditional radial basis function with fixed center and width. The proposed RNN adaptive controller uses a radial basis function with an internal feedback loop and tunes the center, width, and feedback gain of the radial basis function. Simulations of the NN and RNN adaptive control systems with five hidden layer neurons for the initial condition ($\phi = 30$ deg and $\dot{\phi} = 10$ deg/s) is shown in Fig. 1. The state responses are shown in Fig. 1a, and the associated control efforts are shown in Fig. 1b. Simulation results show that the tracking performance is considerably improved by using the proposed RNN adaptive control system.

V. Conclusions

In this Note, an RNN adaptive control system is proposed to control a wing-rock motion system. This Note has successfully demonstrated that the adaptive technique has been applied for the design of an RNN system. This RNN adaptive controller can be applied to a completely unknown system dynamic function. The adaptive laws based on the Lyapunov stability theorem can automatically adjust the interconnection weights of the RNN. Thus, the stability of the developed RNN adaptive control system can be guaranteed. Simulation results have demonstrated that the proposed RNN adaptive controller can achieve favorable control performance for the wing-rock motion system.

Acknowledgments

This work was supported by the National Science Council (NSC) of the Republic of China under Grant NSC 90-2213-E-155-016. The authors are grateful to the reviewers and to the Associate Editor for their valuable comments.

References

[1]Konstadinopoulos, P., Mook, D. T., and Nayfeh, A. H., "Subsonic Wing Rock of Slender Delta Wings," *Journal of Aircraft*, Vol. 22, No. 3, 1985, pp. 223–228.

[2]Elzebda, J. M., Nayfeh, A. H., and Mook, D. T., "Development of an Analytical Model of Wing Rock for Slender Delta Wings," *Journal of Aircraft*, Vol. 26, No. 8, 1989, pp. 737–743.

[3]Nayfeh, A. H., Elzebda, J. M., and Mook, D. T., "Analytical Study of the Subsonic Wing-Rock Phenomenon for Slender Delta Wings," *Journal of Aircraft*, Vol. 26, No. 9, 1989, pp. 805–809.

[4]Singh, S. N., Yim, W., and Wells, W. R., "Direct Adaptive and Neural Control of Wing-Rock Motion of Slender Delta Wings," *Journal of Guidance, Control, and Dynamics*, Vol. 18, No. 1, 1995, pp. 25–30.

[5]Monahemi, M. M., and Krstic, M., "Control of Wing-Rock Motion Using Adaptive Feedback Linearization," *Journal of Guidance, Control, and Dynamics*, Vol. 19, No. 4, 1996, pp. 905–912.

[6]Lee, C. H., and Teng, C. C., "Indentification and Control of Dynamic Systems Using Recurrent Fuzzy Neural Networks," *IEEE Transactions on Fuzzy Systems*, Vol. 8, No. 4, 2000, pp. 349–366.

[7]Wang, L. X., *Adaptive Fuzzy Systems and Control—Design and Stability Analysis*, Prentice–Hall, Englewood Cliffs, NJ, 1994, pp. 140–154.

Angular Velocity Determination Directly from Star Tracker Measurements

John L. Crassidis*
University at Buffalo, State University of New York, Amherst, New York 14260-4400

Introduction

STAR trackers are increasingly used on modern day spacecraft. With the rapid advancement of imaging hardware and high-speed computer processors, current trackers are small and routinely achieve arc-second attitude accuracy.[1] Typical sampling rates for these trackers range from 1 to 10 Hz. As computer processor technology advances, these frequencies will increase, leading to filter designs that provide even more accurate results.

The body angular velocity can be derived using a derivative approach in the attitude kinematics model. For example, if the attitude quaternion $\boldsymbol{q}$ and its derivative $\dot{\boldsymbol{q}}$ (which is usually approximated by a finite difference of the attitude) are known then the angular velocity $\boldsymbol{\omega}$ can be computed from the kinematics equation, with $\boldsymbol{\omega} = 2\Xi^T(\boldsymbol{q})\dot{\boldsymbol{q}}$, where $\Xi(\boldsymbol{q})$ is a 4×3 matrix function of the quaternion (see Ref. 2 for more details). However, this approach requires knowledge of the attitude, which is determined from the star reference and body measurement vectors. In this Note a new and simple approach to determine the angular velocity is shown that depends only on knowledge of the body vector measurements, which are obtained directly from the star tracker. Therefore, angular velocities can still be determined in the event of star pattern recognition anomalies. Also, these velocities can be used to control the spacecraft in the event of gyro failures.

Angular Velocity Determination

In this section a least-squares approach is used to determine the angular velocity from star tracker body measurements

Received 10 December 2001; revision received 31 May 2002; accepted for publication 25 June 2002.

*Associate Professor, Department of Mechanical and Aerospace Engineering. Senior Member AIAA.